Single-Molecule and Single-Nanoparticle SERS: Examining the Roles of Surface Active Sites and Chemical Enhancement

William E. Doering and Shuming Nie*

Department of Chemistry, Indiana University, Bloomington, Indiana 47405

Received: May 7, 2001; In Final Form: October 25, 2001

Recent research in several groups has identified a new class of metal colloidal nanoparticles that is able to enhance the efficiencies of surface-enhanced Raman scattering (SERS) by as much as $10^{14}-10^{15}$ fold. This enormous enhancement allows single-molecule detection and spectroscopy at room temperature. Previous single-molecule and single-particle studies have yielded important insights into the mechanism of electromagnetic field enhancement, but little is known about the contributions of surface active sites and chemical enhancement. Here we report a direct examination of chemical enhancement by using an integrated flow injection and ultrasensitive optical imaging/spectroscopy system. A key feature is that colloidal silver nanoparticles are immobilized on a glass surface inside a microflow device and that single-particle SERS signals are observed in real time while the immobilized particles are treated by chemical reagents in the flow cell. In situ surface plasmon scattering studies of spatially isolated particles indicate that their electromagnetic properties do not change after chemical treatment. Thus, the observed SERS spectral changes should primarily come from chemical enhancement at surface active sites. Our experimental data reveal that three halide ions (Cl^-, Br^-, and I^-) have a substantial activating effect, whereas other ions such as citrate, sulfate, and fluoride have little or no effect on single-particle SERS. A "quenching" effect is observed for thiosulfate ions, which completely destroys the SERS activity. The chemical enhancement factors are estimated to be about 10^2-10^3 for rhodamine 6G molecules adsorbed on single Ag nanoparticles

Introduction

The observation of single-molecule surface-enhanced Raman scattering (SERS) has generated considerable interest both in the nanomaterials community and in the single-molecule spectroscopy community.[1] Following the initial reports of Kneipp, Nie, and their co-workers,[2,3] independent research in several groups[4−7] has confirmed the enormously large enhancement factors on the order of $10^{14}-10^{15}$. A novel finding is a class of optically "hot" nanoparticles that is unusually efficient for optical enhancement.[3,8] Furthermore, spatially isolated single particles and single aggregates have been shown to emit intense bursts of Stokes-shifted photons in an intermittent on−off fashion.[3−6] These results represent a dramatic example in which rare nanostructures with specific optical properties are selected from a large heterogeneous population for correlated spectroscopic and structural studies. Such single-particle studies are expected to yield new insights into both the mechanisms of SERS and the optical properties of nanostructured materials.

At the present, however, it is unclear what mechanisms and structural factors are responsible for single-molecule and single-particle SERS. On the basis of previous SERS studies in bulk samples, it is believed that both a long-range electromagnetic (EM) effect and a short-range chemical effect are simultaneously operative.[9] Schatz[10] discussed the EM mechanism and its dependence on large scale features (10−100 nm), whereas Otto et al.[11] analyzed chemical enhancement and its dependence on atomic scale roughness. Moskovits and co-workers[12] developed a resonant fractal theory to explain surface Raman enhancement in extensively aggregated colloids. The EM mechanism arises from optical excitation of surface plasmon resonances in small metal particles, which leads to a significant increase in the electromagnetic field strength at the particle surface. In the chemical mechanism, molecules adsorbed at certain surface sites (such as atomic clusters, terraces, and steps) are believed to couple electronically with the surface, leading to an enhancement effect similar to resonance Raman scattering.

At the single-particle level, recent theoretical work by Xu et al.[13] suggests that the maximum enhancement factor through electromagnetic fields is about 10^{11}. This enhancement is obtained only at the interstitial sites between two particles or at locations outside sharp surface protrusions. Experimental studies by Brus and co-workers[4] reveal that single-molecule SERS is not strongly correlated with surface plasmon resonance and that the active sites are likely located at the junction between two Ag nanocrystals. This lack of direct correlation suggests that, in addition to the EM component, there is a chemical or related mechanism that is not dependent on the electromagnetic field effect. In other words, surface plasmon excitation is necessary but not sufficient for observing single-molecule SERS. A further finding that cannot be explained by the EM mechanism alone is "blinking SERS", as briefly noted above.[3−6] This phenomenon is superficially similar to intermittent fluorescence emission that has been reported for single-quantum systems such as single fluorescent dye molecules and single semiconductor nanocrystals.[14−17] However, an important difference is that the SERS spectra show considerable fluctuations in both signal intensities and frequencies even under conditions where many molecules are expected to adsorb on a single particle or a single aggregate.[5] A hypothesis is that the "many-molecule" SERS spectra are still dominated by single molecules that are adsorbed

* To whom correspondence should be addressed. E-mail: nie@indiana.edu.

10.1021/jp011730b CCC: $22.00
Published on Web 12/14/2001

at special surface sites or are located at a junction site between two particles.

In this paper, we report a direct examination of the chemical enhancement effect for spatially isolated single nanoparticles. The experimental design involves immobilizing colloidal nanoparticles on a glass surface inside a microflow device and introducing chemical reagents to these particles by flow injection. Single-particle SERS signals are observed continuously on an inverted microscope, whereas various chemical reagents are used to activate or deactivate the chemical enhancement effect. Surface plasmon scattering results indicate that the particle's electromagnetic properties do not change after chemical treatment. Thus, we believe that the chemical and electromagnetic enhancement effects can be separated for single nanocrystals and single nanoaggregates. We show that halide ions are able to increase the SERS intensities of rhodamine 6G, whereas thiosulfate ($S_2O_3^{2-}$) completely destroys the SERS activity. Based on our analysis of the signal-to-noise ratios, we estimate that the chemical enhancement factors achieved on single particles are at least 10^2-10^3. Our results provide evidence that surface active sites play an important role in single-molecule SERS and that these sites are likely associated with residual silver cations and are stabilized by halide ions.

Experimental Section

Colloid Preparation. Silver colloids were prepared according to the standard citrate reduction of Lee and Meisel.[18] Silver nitrate (45 mg) was added to approximately 250 mL of ultrapure water (18 MΩ) and brought to boiling under vigorous magnetic stirring. Upon boiling, 5 mL of a 35 mM sodium citrate solution (1% sodium citrate dihydrate by weight) was injected. The resulting solution was refluxed for 1 h. The greenish-brown sol was ready for use upon cooling. Before immobilization, the sol was incubated for 1−2 h with R6G at a final concentration of 2 nM. After a 10-fold dilution, silver nanoparticles were immobilized by allowing a 40 μL aliquot of the sol to evaporate onto a freshly cleaned cover glass. This dilution step reduced the particle density on the glass surface and was useful in obtaining spatially isolated single particles, but it did not change the single-particle SERS signals in the flow cell. After evaporation, the glass was rinsed exhaustively with water to remove loosely bound particles, and blown dry under a jet of nitrogen. All solutions were prepared in a buffer of 0.7 mM sodium citrate (0.02 wt % sodium citrate dihydrate), to mimic the conditions under which the sol was incubated. Additionally, all solutions contained 2 nM R6G to maintain the adsorption/desorption equilibrium between adsorbed and free R6G molecules.

Microflow Device. For direct observation of single nanoparticles with a high-numerical aperture objective (×100, NA = 1.25), we constructed a custom, stainless steel microflow device with a thin, removable glass window (cover slip). After the colloidal nanoparticles were immobilized on this cover glass, the flow device was assembled and mounted on the microscope stage (Figure 1). The bottom plate of the flow cell was the circular faceplate of the microscope stage. This design allowed a 100× oil-immersion objective to come into contact with the glass window. The flow cell chamber was produced by cutting a hole into a piece of neoprene rubber (1 mm thick). The inlet and outlet were bored into the top piece of the cell such that conventional tubing and connectors (PTFE, 0.0625 in. o.d., 0.030 in. i.d., GlobalFia) could be used. Compressing the top and bottom plates sealed the cell. The final volume of the cell chamber was approximately 0.3 mL. A syringe pump was used to drive solution through the cell. This pulse-free system allowed optical images to be obtained at any time during the experiment without having to stop the liquid flow.

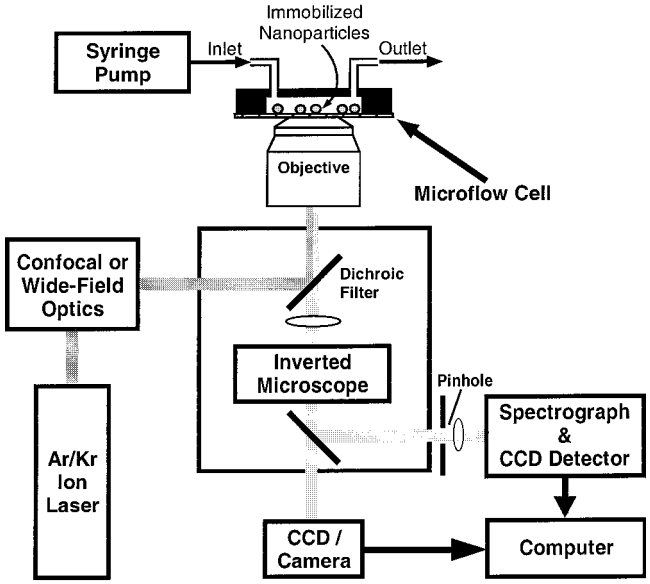

Figure 1. Schematic diagram of the integrated flow-injection and optical imaging/spectroscopy instrument for continuous observation of single-particle SERS. The immobilized nanoparticles were exposed to different chemical reagents by flow injection. See the text for detailed discussion.

Raman Imaging and Spectroscopy. Wide-field optical images were obtained with an inverted optical microscope (Diaphot 200, Nikon). The 514.5 nm line from a mixed gas Ar/Kr ion laser (Lexel 3500) was used for excitation. Backscattered Raman signals were collected through a microscope objective (Plan 100×, oil immersion, NA = 1.25, Nikon). A band-pass filter (540 DF40, Chroma) was used to block the laser line and extraneous signals. Areas of interest were screened in the microscope field of view, and wide-field images were collected with a thermoelectrically cooled CCD (TKB512, Princeton Instruments) or a digital color camera (D1, Nikon) attached to the front port of the microscope. Spectroscopic data were obtained by attaching the CCD detector to a single-stage spectrometer (270M, Spex, Edison, NJ). Statistical data were extracted from wide-field CCD images. Particle-counting software (Scion Image, Scion Corp.) was used to analyze the images by (1) recording the intensity of each nanoparticle, (2) dividing the sum of the particle intensities by the number of particles (yielding an average intensity), and (3) normalizing the average particle intensities after activation against the initial value (e.g, the average signal intensity before activation). This procedure allowed us to correct for the particle-density differences on the glass surface and to compare the relative Raman enhancements among different anions.

Surface Plasmon Resonance Scattering. Surface plasmon resonance images were obtained using an Olympus IX70 inverted microscope in the dark field. White-light illumination was provided by a 100 W halogen lamp. A high-numerical aperture dark-field condenser (U-DCW, Olympus) was used in conjunction with a matching objective (100×, NA = 1.25) to view the particles. The nanoparticles were diluted 5-fold and were immobilized electrostatically using polylysine-coated cover glass. After halide ion activation, the colloidal particles were sandwiched between two coverslips for dark-field microscopy. The flow cells could not be used because it was not compatible

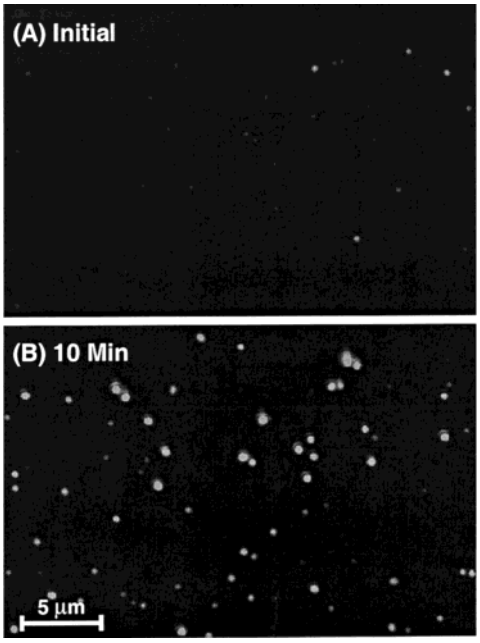

Figure 2. Surface-enhanced Raman scattering images of single immobilized silver nanoparticles before and after 10 min of bromide treatment (panels A and B). The sample was illuminated using 514.5 nm light in a wide-field epi configuration. Total power at the sample was ~50 mW. The camera's exposure time was 10 s. The bromide concentration was 10 mM.

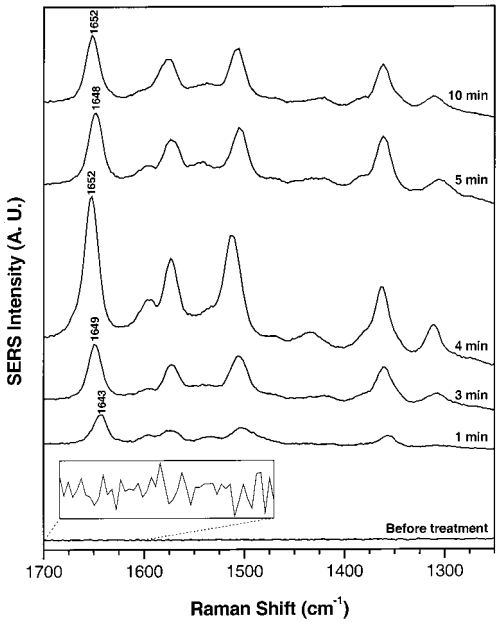

Figure 3. Surface-enhanced Raman scattering spectra of rhodamine 6G obtained from a single nanoparticle at various times of bromide (10 mM) treatment. In each spectrum, the most intense peak at ca. 1650 cm^{-1} is labeled in order to show spectral wandering (frequency jumps). Single-particle spectra were acquired in the confocal mode with ~1 μW 514.5 nm laser excitation and 10 s integration.

with the configuration of dark-field illumination. Dark-field images were captured by using a color digital camera (D1, Nikon).

Results and Discussion

Activation by Halide Ions. Chloride and other halide ions have been known to activate Ag colloids and to increase surface-enhanced Raman scattering in bulk samples.[19] To gain new information that is not available from population-averaged measurements, we have examined this activation effect at the single-particle level. Figure 2 shows surface-enhanced Raman scattering images of single immobilized Ag particles before and after bromide treatment. After 10 min of treatment, both the number of SERS-active particles and the brightness level increased by 5−10 times. A surprising finding is that the dim particles visible before treatment are often not correlated with the bright particles after treatment. An explanation is that the observed particle intensities before halide activation often do not correspond to the actual SERS signals of rhodamine 6G. Because the band-pass filter used in our wide-field imaging passes Stokes-shifted light over a broad spectral range (540−580 nm), the single-particle signals observed in Figure 2 could come from a combination of inelastic background scattering, SERS of rhodamine 6G, SERS of citrate ions, and impurity fluorescence.

To determine the true chemical enhancement factors obtained upon bromide activation, we studied the SERS spectra of rhodamine 6G as a function of treatment time. Figure 3 is an example of the typical SERS spectra obtained from a single particle. Though the nanoparticle is scattering light before treatment, the SERS spectrum shows only a broad background with no detectable Raman signals of R6G. About 1 min after treatment, the rhodamine 6G signals become very clear. Furthermore, the time-elapsed spectra exhibit spectral wandering: the intense SERS peak at 1643 cm^{-1} jumping to 1649, 1652, 1648, and 1652 cm^{-1} with time. These frequency fluctuations are characteristic of single-molecule SERS.[3−6] At 2×10^{-9} M, we estimate that there are about 12 R6G molecules per particle. It is thus interesting that the SERS spectra under such "many-molecule" conditions appear to arise from single molecules adsorbed at special surface sites. In agreement with this interpretation, Kall and co-workers recently reported similar results for tyrosine under many-molecule conditions.[5b]

Before bromide treatment, the background noise (root-mean-square) is calculated to be about 10 counts. Because no Raman signals could be identified for R6G (see inset in Figure 3), we assume that the R6G signals are totally buried in the background and are no larger than the root-mean-square noise. After treatment, the SERS signals of R6G usually increase from ~1000−10 000 counts. These values correspond to chemical enhancement factors on the order of 10^2-10^3. In the future, a more accurate estimate could be made by integrating the SERS signals over a long period of time, which might yield detectable SERS signals before chemical treatment.

In addition to absolute enhancement factors, it is important to discuss the relative activation efficiencies observed for different halide ions. At the single-particle level, iodide ions show a larger chemical enhancement than chloride ions, in agreement with the result of Macklin.[20] In contrast to the bulk data of Hildebrandt and Stockberger,[19] we observed no activation by fluoride ions. Because our particles were securely immobilized, it was not possible for them to aggregate. In traditional bulk studies, fluoride ions are likely to cause colloid aggregation and thus lead to higher SERS intensities. We note that fluoride is the only halide tested which does not form an insoluble salt with the singly charged silver cation. It is also the only halide that is not capable of providing chemical enhancement in our experiment.

The typical time length for activation is on the order of 10−30 min. Often with a lag time of 1−2 min, the particles begin to become more intense and more SERS-active particles appear. The full effect seems to correlate with the stability of the silver-halide complexes. Chloride activated particles usually reach their

maximum intensities within 10 min, whereas bromide takes about 20 min, and iodide takes still longer. Interestingly, the chloride activated particles begin to "decay" shortly after their maximum intensities are reached. Bromide and iodide activated particles remain SERS-active for an extended period of time, with little or no decay after 90 min of treatment. This time-dependent behavior is likely associated with the kinetics of active site formation (see sections below), but the exact reasons remain unclear.

In addition to halide ions, we investigated a number of other species in order to determine whether they might play an important role in SERS. The first study was to use the standard citrate buffer (0.7 mM) without any added salts. The results (not shown) indicate that citrate does not play an activating or deactivating role. Excess citrate molecules adsorbed in the particle surface can produce a weak Raman spectrum, but they do not lead to enhancement of other adsorbed species. Similarly, sulfate does not have an effect on the SERS spectrum of R6G. In previous bulk studies,[21] strong electrolytes have been observed to dramatically increase SERS spectra by salt-induced colloid aggregation.

Deactivation by Thiosulfate Ions. Otto et al.[11] first suggested that the SERS-active sites are associated with residual silver cations and atomic defects on the particle surface. For this reason, some studies have focused on the selective removal of cationic silver. The reagent of choice is thiosulfate, which has long been used as a fixative agent in black and white photography. Thiosulfate "fixes" images by removing cationic silver as a water-soluble silver complex, while leaving neutral silver atoms intact. It has been shown to decrease the SERS intensity on silver electrodes,[22] as well as in AgBr and AgCl colloids.[23,24] At the single-particle level, Figure 4 shows a dramatic decrease in the number of SERS-active nanoparticles after only a few minutes of thiosulfate treatment. All of the SERS-active particles disappeared after 10−30 min of treatment. This supports the notion that surface active sites are at least partially dependent on the presence of silver cations or adatoms.

Electromagnetic vs Chemical Enhancement. A major problem in studying the mechanisms of SERS has been the difficulties in separating the chemical enhancement effect from the electromagnetic field effect. A natural question thus arises: How can one be certain that the immobilized nanoparticles do not undergo significant structural changes (such as aggregation and surface modification) after chemical treatment? Such processes could result in major changes in the electromagnetic field enhancement, in addition to changes in chemical enhancement. To address this question, we have used dark-field microscopy to monitor the surface plasmon scattering properties of single particles before and after chemical treatment. The result shows that neither bromide nor thiosulfate produce detectable changes in surface plasmon scattering (both color and intensity) after 25 min of treatment (Figure 5). As mentioned above, surface plasmon scattering provides an excellent measure of the electromagnetic properties of single and aggregated colloidal nanoparticles. We believe that the observed activation/deactivation effect is primarily due to atomic-scale changes on the particle surface and not large-scale changes that would change the electromagnetic characteristics of the particles. Further wavelength-resolved studies of single-particle plasmon scattering could show small changes (5−10 nm) in the scattering spectra, but such small shifts are unlikely to cause significant changes in electromagnetic enhancement. In fact, previous studies have shown that the surface plasmon spectra are usually very broad and that single-molecule SERS is not directly correlated with surface plasmon scattering.[4]

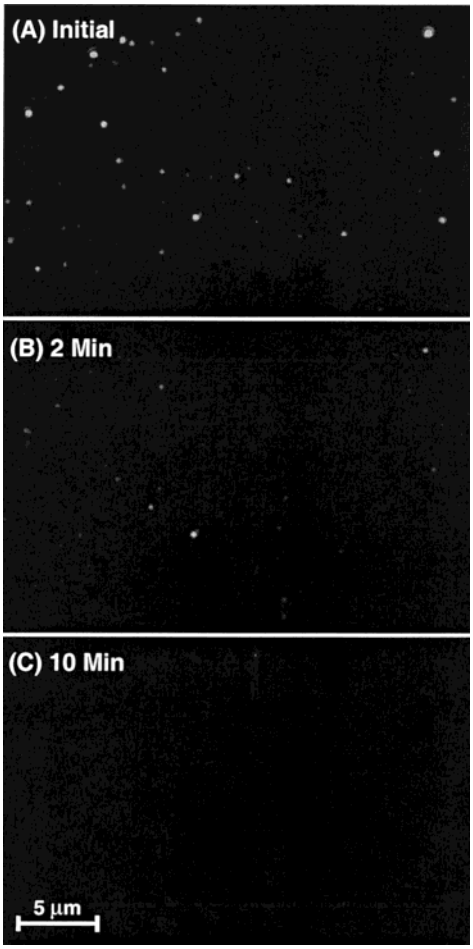

Figure 4. SERS images of single immobilized silver nanoparticles (A) before, (B) after 2 min, and (C) after 10 min of treatment with 10 mM thiosulfate. The experimental conditions were the same as in Figure 2.

Furthermore, we believe that the phenomenon of "blinking SERS" arises from chemical enhancement and not from electromagnetic enhancement. The rationale is that the electromagnetic properties of single nanoparticles cannot change in a random, abrupt fashion. Laser-induced heating is not expected to produce a large enough change in the optical constants of silver.[25] Consistent with this analysis, recent experimental studies have shown that the intensity and color (frequency) of single-particle surface-plasmon scattering do not change with continuous light excitation.[26]

On the other hand, one would expect chemical treatment to directly influence the blinking behavior of single-particle SERS. Indeed, bromide and iodide treatments were found to alter the light emission behavior for most nanoparticles, with the "on" times becoming longer. One hypothesis is that blinking SERS arises from fluctuating active sites (e.g., surface diffusion, R6G desorption, and adsorbate−particle interaction), which are stabilized by bromide and iodide ions. Another possibility is that R6G molecules are slowly accumulated on the particle surface, which would reduce the blinking effect because of population averaging. However, the SERS signal intensities did not increase after extended periods of R6G incubation, ruling out the possibility of R6G accumulation.

Surface Active Sites. A key remaining question is the structure and properties of active sites on the particle surface.

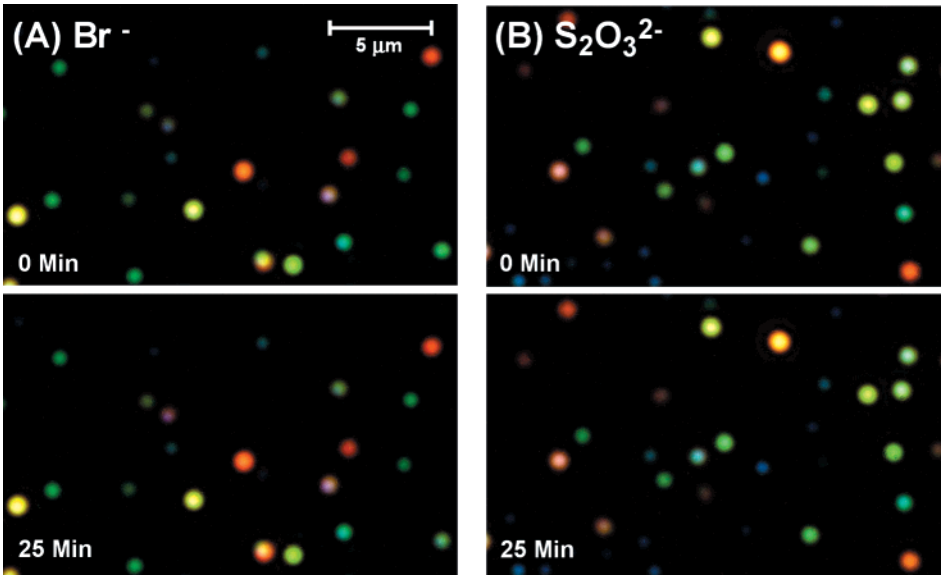

Figure 5. Surface plasmon resonance scattering images of single immobilized nanoparticles before and after chemical treatment. Panel A shows particle scattering images before and after treatment with 10 mM bromide, whereas panel B shows particle scattering images before and after treatment with 10 mM thiosulfate. Note that no changes in scattering intensity or color were observed for any of the immobilized particles (either SERS active or inactive).

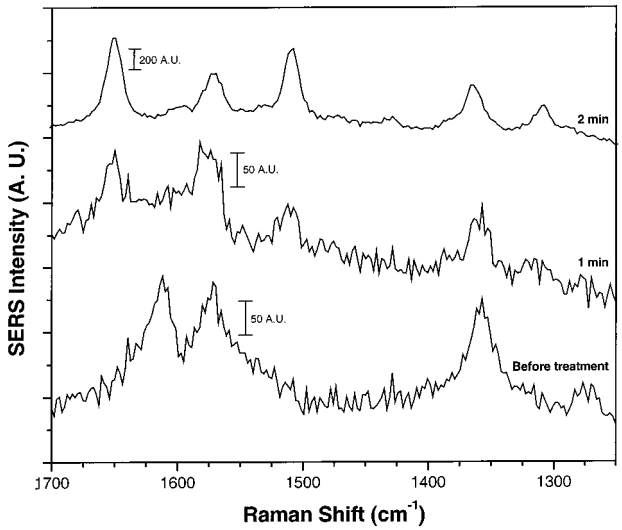

Figure 6. Time-dependent SERS spectra obtained from a single particle, showing the sudden replacement of a citrate background spectrum by the rhodamine 6G spectrum. The single-particle spectra were obtained with a confocal laser beam (~1 μW at 514 nm) prior to bromide treatment and after 1 and 2 min of treatment. The bromide concentration was 10 mM, and the integration time was 10 s.

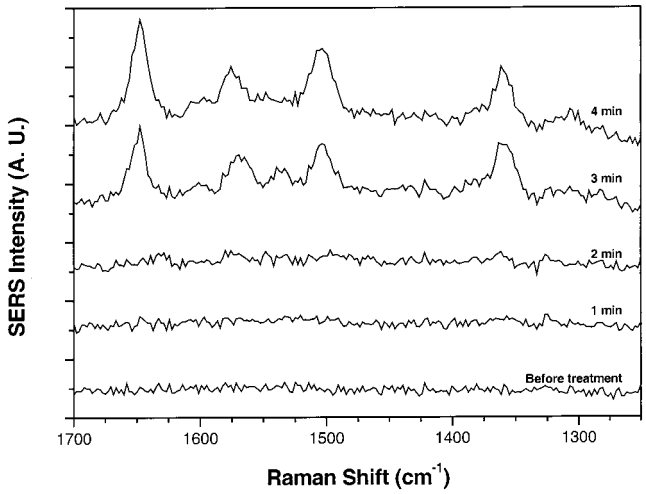

Figure 7. Time-dependent SERS spectra obtained from a single particle, showing the sudden appearance of the rhodamine 6G spectrum after a 2 min lag. Single-particle spectra were obtained with a confocal laser beam (~1 μW at 514 nm) prior to bromide treatment and after 1−4 min of treatment. The bromide concentration was 10 mM, and the integration time was 10 s.

Previous studies suggest that these sites are likely to be adatoms, atomic clusters, sharp steps, or edges.[11] They are responsible for chemical enhancement via resonant charge-transfer and resonance Raman-like enhancement.[27] In other words, strong electronic coupling between an adsorbed molecule and an active site generates new metal-to-ligand or ligand-to-metal charge transfer states that can be broadly excited at visible wavelengths. Previous work by Hildebrandt and Stockburger[19] suggests that the SERS-active sites are high-affinity binding sites (65 kJ per mole) associated with adsorbed anions such as Cl^- or Br^-.

To provide further insight into the nature of active sites, we have used our integrated flow-injection and spectroscopy system to study the replacement of one adsorbed molecule by another. A key observation is that before halide treatment the SERS spectrum often contains a broad background and weak signals from citrate (or its degradation products)[28] but no detectable R6G signals. Upon halide addition, we found that the R6G spectrum suddenly replaces the citrate spectrum and appears over the background in a single step (Figures 6 and 7). The R6G signals then grow over a period of 10−30 min. This replacement behavior is consistent with the conclusion that the SERS spectrum is dominated by a single or a few molecules adsorbed at active sites. Furthermore, the results suggest that the active sites are initially empty or are occupied by citrate ions. The adsorption of halide ions facilitates the subsequent adsorption of R6G but prevents the adsorption of citrate ions at the active sites.

The slow kinetics of halide activation and SERS intensity growth cannot be explained by simple adsorption of halides ions, followed by an accumulation of more R6G molecules on the particle surface. As noted above, the observed spectral fluctuations are characteristic of single-molecule behavior, and the SERS spectrum is dominated by a single or a few molecules

(even though many molecules are present on the particle surface). A possible explanation is that halide ions are able to induce slow structural changes by forming stable complexes with residual Ag cations or adatoms on the particle surface. These structural changes could be considered a "cleaning" effect, leading to stronger R6G adsorption and more efficient enhancement at the active sites. The adsorbed R6G molecules strongly couple with the metal particle, and this interaction results in new electronic states for resonant enhancement. Blinking could be explained by a slow temporal interruption of the electronic coupling between the adsorbed molecule and the metal particle. This model is consistent with the charge-transfer SERS results published in the literature.[1,9] For example, it is well-known that the SERS spectra of pyridine and bipyridine are shifted to higher frequencies (close to those of pyridinium cation), with respect to those observed in normal Raman scattering spectra of bulk pyridine and bipyridine.[22,29,30] This intriguing observation could be explained by surface active sites that are positively charged (like Ag^+).

Because of its similarities to the resonance Raman effect, chemical enhancement is expected to be molecule specific.[31,32] Indeed, we observed a strong activation effect for rhodamine 6G and similar dyes, but not for citrate or water molecules. Further studies need to include pyridines, thiols, and other organic molecules, which will allow us to determine whether SERS activation applies to these compounds under nonresonant excitation conditions.

Single Particles vs Aggregates. Recent results from both Kall's group and Brus's group indicate that the active sites for single-molecule SERS are likely located at the junction between two single particles.[4,5] The experimental evidence is that the optically "hot" particles are frequently aggregates consisting of two or more particles. Because of the restricted configuration of our microflow cell, we were unable to obtain high-resolution AFM or TEM images from the SERS-active particles. Thus, it is possible that the halide-activated "hot" particles observed in this study are also aggregates. However, this situation does not change the main points discussed above, because real-time surface plasmon imaging reveals that all of the particles (singles and aggregates) are stable during chemical treatment. That is, the aggregates do not undergo large structural changes that would be measured by surface plasmon scattering. The chemical nature of the active sites remains the same, whether these sites are located at the junction of two particles or just outside a sharp surface protrusion. Regardless of the exact structure of the "hot" particles (singles or aggregates), our results indicate that chemical enhancement at surface active sites plays an important role in single-molecule and single-particle SERS.

Conclusion

We have reported an integrated flow injection and optical imaging system for examining surface active sites and chemical enhancement in single-molecule SERS. This experimental design allows real-time optical studies of single particles while chemical reagents are introduced to change the atomic structures on the particle surface. We find that the electromagnetic properties of the single immobilized particles (and aggregates) do not change after chemical treatment. As a result, the spectral changes observed after chemical treatment are believed to arise primarily from chemical enhancement at active sites and not from changes in the electromagnetic field effect. The experimental results indicate that three halide ions (Cl^-, Br^-, and I^-) have a substantial activating effect, whereas other ions such as citrate, sulfate, and fluoride have little or no effect on single-particle SERS. In contrast, the photographic fixing agent thiosulfate can efficiently "quench" the SERS signals.

We also estimate that the chemical enhancement factors achieved on single particles are on the order of 10^2-10^3. With the electromagnetic mechanisms contributing to $\sim 10^{11}$ enhancement[13] and the chemical mechanism contributing 10^2-10^3, the total enhancement factors can be expected to be $10^{13}-10^{14}$, in close agreement with the experimental values. On the basis of these and related results, we hypothesize that the surface active sites for single-molecule SERS consist of three components: a single adsorbed molecule, a silver cation, and one or more halide (or other) anions. This model provides a conceptual framework for future experimental and theoretical studies that could ultimately elucidate the mechanisms of surface Raman enhancement. Further studies should also establish SERS as a powerful tool for single-molecule and single-site vibrational spectroscopy.

Acknowledgment. This work was supported by grants from the Department of Energy (DOE FG02-98ER14873) and the National Institutes of Health (R01 GM58173). We are grateful to Mr. Douglas Stuart and Dr. Mingyong Han for technical help in obtaining the dark-field surface plasmon scattering data.

References and Notes

(1) For recent reviews, see: (a) Kneipp, K.; Kneipp, H.; Itzkan, I.; Dasari, R. R.; Feld, M. S. *Chem. Rev.* **1999**, *99*, 2957−2976. (b) Campion, A.; Kambhampati, P. *Chem. Soc. Rev.* **1998**, *27*, 241−250.

(2) Kneipp, K.; Wang, Y.; Kneipp, H.; Perelman, L. T.; Itzkan, I.; Dasari, R. R.; Feld, M. S. *Phys. Rev. Lett.* **1997**, *78*, 1667−1670.

(3) Nie, S.; Emory, S. R. *Science* **1997**, *275*, 1102−1106.

(4) (a) Michaels, A. M.; Nirmal, M.; Brus, L. E. *J. Am. Chem. Soc.* **1999**, *121*, 9932−9939. (b) Michaels, A. M.; Jiang, J.; Brus, L. E. *J. Phys. Chem. B* **2000**, *104*, 11965−11971.

(5) (a) Xu, H.; Bjerneld, E. J.; Kall, M.; Borjesson, L. *Phys. Rev. Lett.* **1999**, *83*, 4357−4360. (b) Bjerneld, E. J.; Johansson, P.; Kall, M. *Single Mol*. **2000**, *1*, 239−248.

(6) Moyer, P. J.; Schmidt, J.; Eng, L. M.; Meixner, A. J. *J. Am. Chem. Soc*. **2000**, *122*, 5409−5410.

(7) Haslett, T. L.; Tay, L.; Moskovits, M. *J. Chem. Phys*. **2000**, *113*, 1641−1646.

(8) (a) Emory, S. R.; Haskins, W. E.; Nie, S. *J. Am. Chem. Soc*. **1998**, *120*, 8009−8010. (b) Emory, S. R.; Nie, S. *J. Phys. Chem. B* **1998**, *102*, 493−497. (c) Krug II, J. T.; Wang, J. D.; Emory, S. R.; Nie, S. *J. Am. Chem. Soc*. **1999**, *121*, 9208−9214.

(9) (a) Van Duyne, R. P. In *Chemical and Biochemical Applications of Lasers*, Moore, C. B., Ed.; Academic Press: New York, 1979; Vol. 4, pp 101−185. (b) Moskovits, M. *Rev. Mod. Phys.* **1985**, *47*, 783−826.

(10) Schatz, G. C. *Acc. Chem. Res.* **1984**, *17*, 370−376.

(11) Otto, A.; Mrozek, I.; Grabhorn, H.; Akemann, W. *J. Phys. Condens. Matter*. **1992**, *4*, 1143−1212.

(12) (a) Douketis, C.; Wang, Z.; Haslett, T. L.; Moskovits, M. *Phys. Rev. B* **1995**, *51*, 11022−11031. (b) Douketis, C.; Haslett, T. L.; Shalaev, V. M.; Wang, Z.; Moskovits, M. *Physica A* **1994**, *207*, 352−359.

(13) Xu, H.; Aizpurua, J.; Kall, M.; Apell, P. *Phys. Rev. E*, **2000**, *62*, 4318−4324.

(14) (a) Trautman, J. K.; Macklin, J. J.; Brus, L. E.; Betzig, E. *Nature* **1994**, *369*, 40−42. (b) Ambrose, W. P.; Goodwin, P. M.; Martin, J. C.; Keller, R. A. *Science* **1994**, *265*, 364−367. (c) Lu, H. P.; Xie, X. S. *Nature (London)* **1997**, *385*, 143−146.

(15) Dickson, R. M.; Cubitt, A. B.; Tsien, R. Y.; Moerner, W. E. *Nature (London)* **1997**, *388*, 355−358.

(16) (a) Vanden Bout, D. A.; Yip, W.-T.; Hu, D.; Fu, D.-K.; Swager, T. M.; Barbara, P. F. *Science* **1997**, *277*, 1074−1077. (b) Yip, W.-T.; Hu, D.; Yu, J.; Vanden Bout, D. A.; Barbara, P. F. *J. Phys. Chem. A* **1998**, *102*, 7564−7575.

(17) (a) Nirmal, M.; Dabbousi, B. O.; Bawendi, M. G.; Macklin, J. J.; Trautman, J. K.; Harris, T. D.; Brus, L. E. *Nature* **1996**, *383*, 802−804. (b) Empedocles, S. A.; Bawendi, M. G. *Science* **1997**, *278*, 2114.

(18) Lee, P. C.; Meisel, D. *J. Phys. Chem.* **1982**, *86*, 3391−3395.

(19) Hildebrandt, P.; Stockburger, M. *J. Phys. Chem.* **1984**, *88*, 5935−5944.

(20) Macklin, J. W. *J. Raman Spectrosc.* **1995**, *26*, 1077−1081.

(21) Nie, S.; Castillo, C. G.; Bergbauer, K. L.; Kuck, J. F. R.; Nabiev, I. R.; Yu, N.-T. *Appl. Spectrosc.* **1990**, *44*, 571−575.

(22) Watanabe, T.; Kawanami, O.; Honda, K.; Pettinger, B. *Chem. Phys. Lett.* **1983**, *102*, 565−570.

(23) Jian, W.; Dawei, L.; Houwen, X.; Xu, S.; Fan-Chen, L. *Spectrochim. Acta* **1987**, *43A*, 375−378.

(24) Dawei, L.; Jian, W.; Houwen, X.; Xu, S.; Fan-Chen, L. *Spectrochim. Acta* **1987**, *43A*, 379−382.

(25) Leung, P. T.; Hider, M. H.; Sanchez, E. J. *Phys. Rev. B*. **1996**, *53*, 12659−12662.

(26) Schultz, S.; Smith, D. R.; Mock, J. J.; Schultz, D. A. *Proc. Natl. Acad. Sci. U.S.A.* **2000**, *97*, 996−1001.

(27) (a) Lombardi, J. R.; Birke, R. L.; Tu, T.; Xu, J. *J. Chem. Phys*. **1986**, *84*, 4174−4180. (b) Kambhampati, P.; Child, C. M.; Campion, A. *J. Chem. Soc., Faraday Trans*. **1996**, *92* (23), 4775−4780.

(28) (a) Munro, C. H.; Smith, W. E.; Garner, M.; Clarkson, J.; White, P. C. *Langmuir* **1995**, *11*, 3712−3720. (b) Siiman, O.; Bumm, L. A.; Callaghan, R.; Blatchford, C. G.; Kerker, M. *J. Phys. Chem*. **1983**, *87*, 1014−1023.

(29) Roy, D.; Furtak, T. E. *Chem. Phys. Lett*. **1986**, *124*, 299−303.

(30) Kim, M.; Itoh, K. *J. Phys. Chem*. **1987**, *91*, 126−131.

(31) Liang, E. J.; Ye, X. L.; Kiefer, W. *J. Phys. Chem. A* **1997**, *101*, 7330−7335.

(32) Wehling, B.; Hill, W.; Klockow, D. *J. Mol. Struct.* **1995**, *349*, 117−120.